Kinetics of Solid−Solid Reactions: Influence of the Number of Contact Points

ARTICLE *in* INDUSTRIAL & ENGINEERING CHEMISTRY RESEARCH · JULY 2014

Impact Factor: 2.59 · DOI: 10.1021/ie501542p

3 AUTHORS, INCLUDING:

Amaresh Raichur
Indian Institute of Technology Bombay/PDA…
5 PUBLICATIONS **7** CITATIONS
SEE PROFILE

A.K. Suresh
Indian Institute of Technology Bombay
71 PUBLICATIONS **1,204** CITATIONS
SEE PROFILE

I&EC research
Industrial & Engineering Chemistry Research

Article

pubs.acs.org/IECR

Kinetics of Solid−Solid Reactions: Influence of the Number of Contact Points

R. Amaresh,† Manan Pathak, and A. K. Suresh*

Indian Institute of Technology Bombay, Powai, Mumbai 400076, India

ABSTRACT: Dalvi and Suresh (*AIChE J.* **2011**, *57*, 1329−1338) proposed a model for the kinetics of a reaction between two particulate solids A and B, where B is the diffusing component, in terms of the average number of contact points N_{AB} between the two types of particles. In the present work, the applicability and validity of the model is studied, taking the formation of tricalcium aluminate from its immediate precursors as a candidate reaction. Partial analytical solutions to the Dalvi−Suresh model have been derived, and a simple parameter-estimation methodology has been developed. The data clearly show an influence of N_{AB}, and use of the Ginstling−Brounshtein model (*Appl. Chem. USSR* **1950**, *23*, 1327−1338) for parameter estimation leads to diffusivity values that depend on N_{AB} in a systematic way. Parameters estimated using the Dalvi−Suresh model, on the other hand, show only a random scatter and also show reasonable agreement with the values of diffusivity of Ca in oxides.

1. INTRODUCTION

Many processes of interest in the metallurgical, chemical, ceramic, and cement industries involve solid−solid reactions. Such reactions are carried out by either intimately mixing the reactant powders or pelletizing the reactant powders together in the desired ratio and bringing the mixed powder/pellets to reaction conditions.[1] Such reactions have usually been treated using models inspired by solid−fluid reactions, which assume continuous contact between the reactants (see Ghoroi and Suresh[1−3] for a review) all around the reacting particle. Because particles in solid mixtures are generally in contact at a finite number of points, it seems more probable, particularly in the pellet situation, that the reaction starts at these contact points and continues by the diffusion of one or both of the reactants through the product phase.[2,4,5] These reaction systems are difficult to understand and model, primarily because of the complex geometries that arise from the many factors that control the kinetics, such as particle size, size distribution, number and distribution of contact points, particle shape, contact area between particles, intermediates formed, vaporization, surface diffusion, and intermediates formed.[3] With some assumptions about the geometry to make the mathematical problem tractable along with the assumption of diffusion control, models were derived in what can be called the contact-point framework by Hao and Tanaka[5] and Dalvi and Suresh.[4] In these approaches, the average number of contact points N_{AB} is estimated from the Ouchiyama−Tanaka[6] equation and assumed to remain constant throughout the reaction. Of the models in this genre, only the Dalvi−Suresh model[4] shows the correct asymptotic behavior in the limit of large N_{AB}.

Few experimental studies in the literature allow a critical validation of the contact-point models, because the data needed for calculation of N_{AB} are often unavailable. Shimizu and Hao[7] and Shimizu[8] compared continuous-contact and contact-point models using the experimental data for several systems and came to the conclusion that the Hao−Tanaka model[5] gave a more consistent value of the diffusivity than shrinking-core-type models. This is surprising, because the number of contact points in the situations they considered was so large that one would expect the continuous-contact models to perform fairly well. However, as pointed out earlier, the Hao−Tanaka[5] model does not approach the continuous-contact asymptote as N_{AB} is increased, and this could have been a reason for the difference. Using data for the calcia−alumina system, Ghoroi and Suresh[1,2] showed the inadequacies of earlier models to explain the reaction kinetics among solid reactants and highlighted the lack of adequate experimental data to validate models for solid−solid reactions, especially those of the contact-point variety.

The purpose of this article is to examine the applicability of the theories developed for solid−solid reactions and, in particular, to investigate the influence of contact points, using experimental data systematically generated for this objective. Along the way, we derive a simple parameter-estimation methodology for the contact-point model of Dalvi and Suresh[4] and validate it against experimental data. The single-step formation of $Ca_3Al_2O_4$ (denoted as C_3A) from $Ca_{12}Al_{14}O_{33}$ (denoted as $C_{12}A_7$) and CaO[2] is the system chosen, and different values of N_{AB} were achieved by varying the particle sizes of the individual reactants. Quantitative X-ray diffraction (QXRD) by full profile fitting[9−11] was used to follow the reaction.

2. THEORY

Consider a reaction between solid particles of A and B, producing a solid product

$$aA + bB \rightarrow \text{product} \quad (1)$$

Assuming that the reaction takes place in a particle of A by diffusion of B, Figure 1 shows the geometry of the reaction zone from a contact point for a partially reacted particle (A), according to the Dalvi−Suresh model. To provide a finite area for diffusion to start, the geometry at the contact point is

Received: April 15, 2014
Revised: June 15, 2014
Accepted: June 18, 2014

dx.doi.org/10.1021/ie501542p | *Ind. Eng. Chem. Res.* XXXX, XXX, XXX−XXX

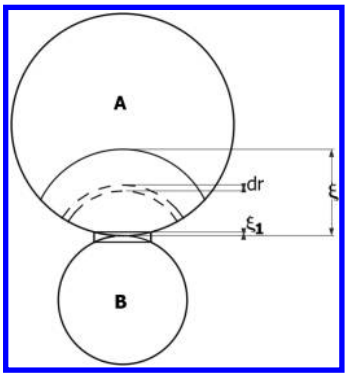

Figure 1. Schematic representation of the geometry of the reacting particle in phase 1, shown for a single contact point.

assumed to be a cylindrical disk, as shown in Figure 1, with a thickness of ξ_1 protruding into the particle of A. In their model, Dalvi and Suresh[4] assumed the reaction to be diffusion-limited and diffusion to proceed strictly in the radial direction from the contact point as the center. ξ is the radius of the product zone at any time, and r refers to any radial position inside the product zone. Clearly, depending on the value of N_{AB}, the product zones for neighboring contact points develop independently of one another (phase 1 of the reaction) until some time at which they touch and, later, overlap. The period after phase 1 is further divided in the model into phase 2 (in which the neighboring product zones overlap partially but the surface of A is still not covered completely by the footprints of the product zones) and phase 3 (in which the surface is completely covered by the footprints of the product zones and, hence, unreacted A is confined to a golf-ball-like core region). Conversion of A is given at any time uniquely by the position ξ of the reaction front (see Dalvi and Suresh[4] for the relevant equations), and the relation between ξ and time is given by the model as

$$\rho_A S(\xi)\frac{d\xi}{dt} = \frac{a}{b}\frac{D\rho_B}{\int_{\xi_1}^{\xi}\frac{dr}{S(r)}} \tag{2}$$

with the initial condition

$$t = 0, \quad r = \xi_1$$

where ρ_A and ρ_B are the molar densities of A and B, respectively, and $S(r)$ is the surface area of a (spherical) section at radius r within the product zone ($\xi_1 \le r \le \xi$). The nature of the function $S(r)$ depends on the phase of the reaction, and the equations for different phases are available from Dalvi and Suresh.[4]

Dalvi and Suresh[4] presented the solution to eq 2 in integral form as

$$I(\xi) = \int_{\xi_1}^{\xi} S(\bar{\xi})\left[\int_{\xi_1}^{\bar{\xi}}\frac{dr}{S(r)}\right]d\bar{\xi} = \int_{\xi_1}^{\xi} S(\bar{\xi})\, i(\bar{\xi})\, d\bar{\xi} = \frac{D}{K}t \tag{3}$$

where $i(\bar{\xi})$ stands for the inner integral in the formulation of Dalvi and Suresh.[4] In this work, $i(\bar{\xi})$ in eq 3 was evaluated analytically for all three phases. The solutions are given in the following subsections.

2.1. Reaction in Phase 1. Phase 1 of the reaction applies for $\xi_1 \le \xi \le \xi_c$, where ξ_c is given by

$$\xi_c = \frac{2r_{A0}\sqrt{N_{AB}-1}}{N_{AB}}$$

Using the appropriate expression for $S(r)$ from Dalvi and Suresh[4] for this phase, one obtains

$$i(\bar{\xi})|_{\text{phase 1}} = \int_{\xi_1}^{\bar{\xi}}\frac{dr}{S(r)} = \frac{1}{2\pi}\int_{\xi_1}^{\bar{\xi}}\frac{dr}{r^2\left(1-\frac{r}{2r_{A0}}\right)} = \frac{1}{4\pi r_{A0}}\left[\ln\frac{\bar{\xi}(2r_{A0}-\xi_1)}{\xi_1(2r_{A0}-\bar{\xi})} + 2r_{A0}\frac{\bar{\xi}-\xi_1}{\xi_1\bar{\xi}}\right] \tag{4}$$

2.2. Reaction in Phase 2. Phase 2 applies for $\xi_c \le \xi \le \xi_c'$, where ξ_c' is given by $\xi_c' = 2r_{A0}/(N_{AB})^{1/2}$.

For this case, one must evaluate the inner integral in two parts[4]

$$i(\bar{\xi})|_{\text{phase 2}} = \int_{\xi_1}^{\xi_c}\frac{dr}{S(r)} + \int_{\xi_c}^{\bar{\xi}}\frac{dr}{S(r)} = i(\xi_c)|_{\text{phase 1}} + \int_{\xi_c}^{\bar{\xi}}\frac{dr}{S(r)} \tag{5}$$

where the first term on the right can be calculated using eq 4. The second integral is

$$\int_{\xi_c}^{\bar{\xi}}\frac{dr}{S(r)} = \frac{-r_{A0}}{\pi}\left\{\frac{-1}{2p\xi_c r_{A0}}\ln\left(\frac{\bar{\xi}}{\xi_c}\right) + \left[\left(\frac{p-1}{4p\xi_c L}\right)\ln\left(\frac{\{\bar{\xi}+[r_{A0}(p-1)]-L\}\{\xi_c+[r_{A0}(p-1)]+L\}}{\{\bar{\xi}+[r_{A0}(p-1)]+L\}\{\xi_c+[r_{A0}(p-1)]-L\}}\right)\right] + \frac{1}{4pr_{A0}\xi_c}\ln\left(\frac{\bar{\xi}^2+[2r_{A0}(p-1)\bar{\xi}-2pr_{A0}\xi_c]}{\xi_c{}^2-2r_{A0}\xi_c}\right)\right\} \tag{6}$$

where $L = [2pr_{A0}\xi_c + r_{A0}{}^2(p-1)^2]^{1/2}$.

2.3. Reaction in Phase 3. Phase 3 applies when $\xi > \xi_c'$. For this situation, one must evaluate $i(\xi)$ as follows[4]

$$i(\bar{\xi})|_{\text{phase 3}} = i(\xi_c')|_{\text{phase 2}} + \int_{\xi_c'}^{\bar{\xi}}\frac{dr}{S(r)}$$

The first term on the right can be calculated using eqs 5 and 6, and the second term evaluates to

$$\int_{\xi_c'}^{\bar{\xi}}\frac{dr}{S(r)} = \frac{1}{2\pi\xi_c r_{A0}}\left\{\left[\frac{2Mr_{A0}}{M-2x(r_{A0}+\xi_c)}\right] - \left[\frac{2Mr_{A0}}{M-2N(r_{A0}+\xi_c)}\right] + \xi_c\left(\ln\left\{\frac{[r_{A0}-\xi_c-Mx+x^2(r_{A0}+\xi_c)](1+N^2)}{[r_{A0}-\xi_c-MN+N^2(r_{A0}+\xi_c)](1+x^2)}\right\}\right) - M[(\tan^{-1}x)-(\tan^{-1}N)]\right\} \tag{7}$$

where

dx.doi.org/10.1021/ie501542p | Ind. Eng. Chem. Res. XXXX, XXX, XXX−XXX

$$M = 2\sqrt{{r_{A0}}^2 - {\xi_c}^2}, \quad x = \sqrt{\frac{\bar{\xi} - \xi_c}{\bar{\xi} + \xi_c}}, \quad N = \sqrt{\frac{\xi_c' - \xi_c}{\xi_c' + \xi_c}}$$

The number of contact points as a function of radius ratio, molar ratio, and density ratio is given by the expression of Ouchiyama and Tanaka,[6] which can be expressed[7] as

$$N_{AB} = \frac{4(1 - \varepsilon_A)(2\gamma + R_r + 1)^2[2R_r + \gamma(R_r + 1)]^2}{[3(\gamma + R_r)^2 + (\gamma + 1)(\gamma + {R_r}^2)](\gamma + {R_r}^2)(\gamma + 1)} \quad (8)$$

where $\gamma = R_\rho {R_r}^3/R_m$. This shows that N_{AB} can be varied for a given mole ratio of the reacting components by changing the sizes of the particles of the two phases involved.

The equations for ξ_c and ξ_c' above show that the (dimensionless) positions of the reaction front at the ends of phases 1 and 2, and hence the conversions achieved, depend only on the value of N_{AB}. The parameter-estimation procedure can therefore be considerably simplified, based on the idea that the conversion range in phase 1 can be extended by choosing small values for N_{AB}, through a suitable choice of particle sizes. From conversion−time data for such systems, the positions of the reaction front, and hence $I(\xi)$ using eq 5, can be evaluated at different times, and parameter estimation can be carried out by linear regression on a plot of $I(\xi)$ versus time in accordance with eq 3. Using such estimates, the fit of the model to data for larger N_{AB} values (for which all three phases of reaction can be seen over the conversion range of interest) can be examined to validate the model over the entire range of conversions.

3. EXPERIMENTAL SECTION

The calcia (C)−alumina (A) system was chosen for the present studies because it has several features that especially suit the objectives of the present work. Previous work[1−3] has shown that, in this system, the reaction takes place in the alumina particle by the diffusion of calcia. The assumption of unilateral diffusion made in the Dalvi−Suresh model[4] is thus satisfied. Ghoroi and Suresh[1] showed that, for this system in the temperature range of 1150−1300 °C, $C_{12}A_7$ forms as an intermediate and the reaction of $C_{12}A_7$ with calcia to form C_3A occurs in a single step. Finally, because the densities of $C_{12}A_7$ and C_3A are comparable, the size of the reacting particle can be assumed to be constant throughout the reaction, another assumption in the Dalvi−Suresh model. Experiments were therefore planned to study the conversion of $C_{12}A_7$ to C_3A and test the applicability of the Dalvi−Suresh model.

Accurate measurements of the amounts of reactant and product phases at different stages of reaction are necessary to follow the kinetics of solid−solid reactions.[2,3] Quantitative X-ray diffraction (XRD) provides a means of doing this.[1,12,13] Whereas previous works[1,12,13] tended to follow the reference intensity ratio (RIR) technique, in this work, we used full profile fitting methods based on Rietveld refinement,[10,11,14] because of their simplicity, their ability to fit the entire profile, and the availability of powerful public-domain software such as MAUD[10−13] and FULLPROF for interpretation. In this technique, the whole XRD pattern is fitted with reference data from crystal databases. The method is widely used in the cement industry but has not been applied in kinetic investigations. It works particularly well when the number of phases in the sample is small, such as when no intermediates are present.

The experimental plan undertaken had four stages: (i) synthesis of pure $C_{12}A_7$ and CaO and their size fractionation to obtain particles of the required size, (ii) mixing and preparation, (iii) execution of kinetic experiments, and (iv) measurement of XRD patterns of reacted samples to determine the conversion−time curves for the experiments. The physical constants of reactants relevant for the present work are given in Table 1. The value of K in eq 3 can be calculated from the values in this table as 0.2909.

Table 1. Physical Constants of Reactants and Product Used in This Work

phase	density[1,2] (kg m^{-3})	molar density (kmol/m^3)	lattice parameter (Å)	volume of unit cell (Å^3)	space group
$C_{12}A_7$	2700	1.94	11.989	1720.67	$I\bar{4}3d$
C_3A	3030	11.34	15.263	3555.65	$Pa\bar{3}$
CaO	3350	59.82	4.8	110.6	$Fm\bar{3}m$

3.1. Synthesis of Pure $C_{12}A_7$ and CaO. Pure $C_{12}A_7$ was synthesized by solid-state reaction using as precursors pure, commercially available $CaCO_3$ and $Al(OH)_3$ in the required stoichiometric ratio at around 1260 °C. The reaction is

$$12CaCO_3 + 14Al(OH)_3 \rightarrow Ca_{12}Al_{14}O_{33} + 21H_2O\uparrow + 12CO_2\uparrow \quad (9)$$

The following protocol for synthesis was established after some initial trials: The required weights of $CaCO_3$ and $Al(OH)_3$ were mixed together and lightly ground in a mortar and pestle to break the agglomerates. Intensive grinding was avoided as it causes additional artifacts such as mechanical activation. Ground and mixed samples were heated at a rate of 10 °C/min to 1260 °C in a high-temperature furnace (Okay furnace, Bysakh & Company, Kolkata, India) and maintained at the final temperature for 2 h. Then, after natural cooling of the furnace, each sample was again lightly ground and heated for around 3 h at the same heating rate as used earlier to a temperature of 1300−1350 °C in the presence of dry air. The reacted samples were checked for completion of the reaction using XRD. Crystallographic information files (CIFs) for CaO, C_3A, and $C_{12}A_7$ from the Inorganic Crystal Structure Database (ICSD) were used for the purpose. A typical result is presented in Figure 2 and shows the existence of a single phase of $C_{12}A_7$ without any CaO or C_3A.

The product was sieved to obtain the required size fractions. All sized samples showed formation of a single phase of cubic hexa-tetrahedral class symmetry ($I\bar{4}3d$) $C_{12}A_7$ with lattice parameter a = 11.95−11.99 Å, with two formula units per unit cell.

Pure CaO for the experiments was also prepared by solid-state reaction from pure commercial $CaCO_3$ precursor at around 1200 °C. The reaction is

$$CaCO_3 \rightarrow CaO + CO_2 \quad (10)$$

The CaO thus obtained was lightly ground and sieved to obtain the desired size (diameter = −38 + 25 μm, average = 31.5 μm). Precaution was taken to maintain an oxidizing atmosphere in the furnace by giving sufficient time for the formed CO_2 to escape, by controlling the heating rate (20 °C/min) and allowing a sufficient soaking time (3 h) at the peak temperature. The CaO thus prepared was immediately utilized after sieving to the

dx.doi.org/10.1021/ie501542p | Ind. Eng. Chem. Res. XXXX, XXX, XXX−XXX

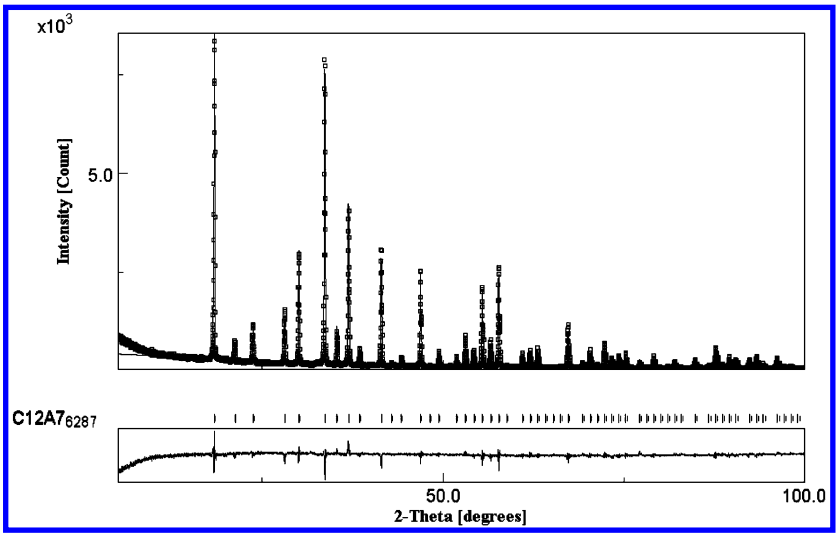

Figure 2. Experimental XRD profiles of synthesized powders fitted by the MAUD program, showing a pure phase of $C_{12}A_7$. The subscript of C12A7 represents the CIF file number from ICSD.

Table 2. Physical Properties of Reactant Powders Used in the Kinetic Study[a]

sample	retaining sieve ("mesh") size (μm)	average radius of $C_{12}A_7$ (r_{A0}, μm)	radius ratio, R_r (r_{B0}/r_{A0})	surface area/volume ratio of $C_{12}A_7$ ($\times 10^5$ m^2/m^3)	N_{AB} (eq 8)
S1	(−38 + 25)	15.75	1.00	1.90	3
S2	(−53 + 45)	24.5	0.65	1.22	6
S3	(−75 + 63)	34.5	0.46	0.87	12
S4	(−90 + 75)	41.3	0.39	0.726	17
S5	(−125 + 106)	57.75	0.276	0.519	41

[a] r_{B0} = 15.75 μm (kept constant for all samples). For samples S1−S4, R_m = 9, and $C_{12}A_7$/C mole ratio = 1:9. For N_{AB} = 41, R_m = 15, and $C_{12}A_7$/C mole ratio = 1:15.

required size to avoid slaking or carbonation. The particle size of CaO was kept constant in all experiments to minimize its handling.

3.2. Mixing and Pellet Preparation. Formation of C_3A from CaO and $C_{12}A_7$ at 1250 °C from solid−solid reaction can be written as

$$C_{12}A_7 + 9CaO \rightarrow 7(3CaO{\cdot}Al_2O_3) \quad (11)$$

Reactants $C_{12}A_7$ and CaO as powders of the required sizes were loaded in an airtight soft polyethylene cylindrical bottle and shaken in all directions randomly for about 25 min for each specimen. The designed mixing process was aimed at obtaining a homogeneous mixture. The time required for mixing was determined after some trials based on the consistency in measured density of specimen pellets pressed from randomly drawn powder mixtures. Twenty minutes was found to be sufficient for achieving uniform mixing according to this criterion. The sizes of $C_{12}A_7$ particles used for different samples along with other properties of interest are provided Table 2. The reactants were taken in stoichiometric proportion in all cases except for N_{AB} = 41, for which an excess of CaO was used.

From the powder mixtures, pellets were prepared by uniaxial hydrostatic pressing at a pressure of 31 MPa. The process of pellet preparation employed was that described by Ghoroi and Suresh.[1]

3.3. Kinetic Experiments. The experimental protocols described in this section were established after several initial trials. All reactions were conducted at a temperature of 1250 °C. Because the reactants were taken in a stoichiometric ratio for four samples among the five analyzed, an upper limit to conversion of 75% was decided so that the effects of exhaustion of the diffusing reactant did not play a role. Pellets with different N_{AB} values were placed in a platinum crucible and loaded in the furnace at 800 °C. The reaction temperature of 1250 °C was attained in 2700 s (45 min). At this point, the pellets were removed, and conversions were measured by XRD. This was taken as the start of the isothermal part of the reaction for the purposes of parameter estimation.

For conversions at other times, a similar procedure was followed. For each time point, specimen pellets with different N_{AB} values were reacted together. Samples were withdrawn at times of 45 (as above), 60, 75, 105, 135, and 165 min. Two cases (N_{AB} = 3 and 17) were used to check the reproducibility of kinetic data. For these cases, two specimens for each N_{AB} value were reacted for certain samples.

3.4. Quantitative Analysis of Samples. The specimens removed from the furnace were quenched and stored in polyethylene bags under a vacuum for QXRD testing. Samples for QXRD were prepared by grinding them in an agate mortar and pestle to pass through a 25-μm sieve. Powder XRD patterns were obtained, as explained by Ghoroi and Suresh,[1] in a PANalytical X'pert X-ray diffraction machine using a Cu anode. The open-source MAUD program was used in the range of $5° \leq 2\theta \leq 70°$ to quantify the amounts of product and reactant phases in the sample. The method was checked for our system before application for the kinetic study using known mixtures of $C_{12}A_7$ and C_3A; the results are reported in Table 3. The (relative) difference between the estimated and actual weight fractions of C_3A in these experiments was seen to vary from 0.25% to 3.43%. As described below, our calculations of

dx.doi.org/10.1021/ie501542p | Ind. Eng. Chem. Res. XXXX, XXX, XXX−XXX

Table 3. Validation of the Conversion Determination Procedure Using Full-Profile XRD Fitting

compound (phase)	actual weight added (g)	actual weight added (%)	weight percentage determined from XRD (using MAUD)	relative error (%)
			Sample 1	
$C_{12}A_7$	0.2348	22.33	22.12 ± 0.41	−0.94
C_3A	0.8163	77.67	77.87 ± 1	+0.25
			Sample 2	
$C_{12}A_7$	0.4065	37.56	36.20 ± 1.89	−3.62
C_3A	0.6756	62.44	63.79 ± 2.64	+2.16
			Sample 3	
$C_{12}A_7$	0.6621	61.03	59.68 ± 2.00	−2.21
C_3A	0.4266	38.97	40.31 ± 1.89	+3.43

conversions were based on a quantification of C_3A, and it can therefore be concluded that quantification of conversions to within about 3−3.5% was achieved by this method in the conversion range tested.

The basics of Rietveld refinement[10,11] and application of the MAUD program for quantitative phase analysis are exhaustively explained in the literature.[10,11,16−19] Obtaining a good XRD pattern is crucial to the success of the method, and fixed instrument parameters and a low scan rate were employed to achieve this. The program uses high-quality standard crystallographic information files (CIFs) from ICSD (file numbers 6287 for $C_{12}A_7$ and 1841 for C_3A were used, externally supplied in the present case) as reference for the peak intensities. After fitting, the densities of fitted CIF files, as returned by the MAUD program, were compared with each other and with known crystal densities as a check for consistency. The variations in density among all samples after refinement were 2683 ± 13.45 kg/m^3 for $C_{12}A_7$ and 3030 ± 3 kg/m^3 for C_3A. These results are within the range of values reported[20,21] for $C_{12}A_7$ (2670−2696 kg/m^3) and C_3A (3161−3362 kg/m^3). The corresponding lattice parameter ranges are 11.95−11.989 Å for $C_{12}A_7$ and 15.25−15.263[21] Å for C_3A.

The weight fraction of the product phase in the sample, W_p, as estimated by the MAUD program,[9] was used to calculate the conversion as follows

$$\alpha = W_p\left(\frac{m_{r0} + m_{C0}}{m_{r0}}\right)\left(\frac{1386}{1890}\right) \tag{12}$$

where m_{r0} and m_{C0} refer to the initial weights of $C_{12}A_7$ and CaO, respectively, taken in the reaction mixture. The last (numerical) factor is the stoichiometric weight ratio between $C_{12}A_7$ consumed and C_3A formed.

4. RESULTS AND DISCUSSION

Figure 3 compares the XRD patterns obtained for samples reacted for different times for one value of N_{AB} (= 17). An increase with time in the peak intensities at 2θ values of ∼33.17° and ∼47.5° was observed, showing an increase in the quantity of C_3A. A simultaneous decrease in peak intensity at $2\theta \approx 18.13°$, indicating a decrease of $C_{12}A_7$, was also seen.

Table 4 lists the mean radii of the reacting particles, the reaction front positions at the end of phases 1 and 2 of reaction (calculated from N_{AB}), and the corresponding conversions for the different values of N_{AB} considered. The choice of N_{AB} values for the experiments was motivated by the following factors: In

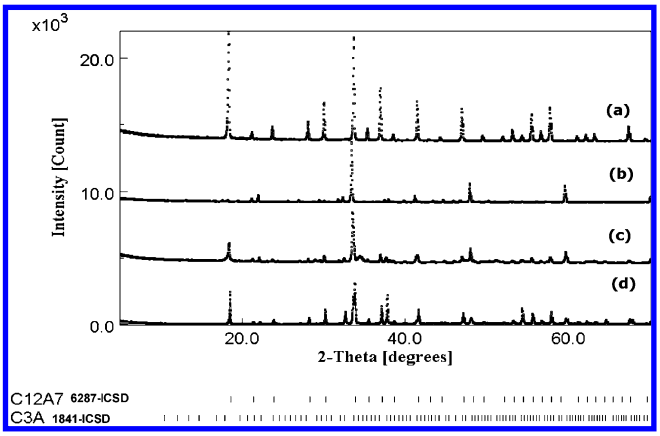

Figure 3. XRD patterns obtained for (a) pure $C_{12}A_7$, (b) pure C_3A, and (c,d) reaction samples for N_{AB} = 17 at (c) 9900 and (d) 2700 s. ICSD files for the pure phases, used to match the experimental profiles, are listed at the bottom left.

Table 4. Calculated Reaction Front Positions and and Corresponding Conversions at the End of Phase 1 of the Reaction for the Different Values of N_{AB} Used in These Studies

N_{AB}	r_{A0}	ξ_c	ξ'_c	α_c	α'_c
3	1.58×10^{-5}	1.36×10^{-5}	1.82×10^{-5}	0.66	0.91
6	2.45×10^{-5}	1.83×10^{-5}	2.00×10^{-5}	0.90	1.00
12	3.45×10^{-5}	1.91×10^{-5}	1.99×10^{-5}	0.80	0.89
17	4.13×10^{-5}	1.94×10^{-5}	2.00×10^{-5}	0.73	0.79
41	5.78×10^{-5}	1.79×10^{-5}	1.81×10^{-5}	0.53	0.55

their article, Dalvi and Suresh[4] made a distinction between small N_{AB} values (up to 4), for which the number of contact points surrounding a given contact point (denoted by p in their article) is exactly known, and the general case, for which they assumed an average value of p = 4. We wanted to test the model for both cases. Further, the values of α_c for N_{AB} values of 6, 12, and 17 are high enough that we expected to have enough data points in phase 1 for parameter estimation. Finally, a high value of 41 provides an opportunity to compare the model predictions, using parameters estimated from lower N_{AB} values, throughout the conversion range encompassing all phases.

The kinetic data obtained are reported in Table 5. The data for N_{AB} = 3 and 17, for certain time points, show the results from repeat experiments and demonstrate the good reproducibility ensured by the experimental protocols.

Figure 4 shows the data plotted as a function of t/r_{A0}^2. The choice of abscissa was inspired by the Ginstling−Brounshtein (GB) equation[15]

$$g(\alpha) = 1 - \frac{2}{3}\alpha - (1-\alpha)^{2/3} = D\left(\frac{2t}{Kr_{A0}^2}\right) \tag{13}$$

according to which such a plot is expected to be independent of N_{AB}. The influence of N_{AB} in Figure 4, however, is clear, and thus, there is immediate support for a contact-point framework in these results.

Next, we used the (phase 1) data for N_{AB} = 6, 12, and 17 for parameter estimation in the Dalvi−Suresh model. Because isothermal conditions could be assumed only for times beyond t_0 = 2700 s, eq 3 was integrated from t_0 to different times (instead of from time 0). This gives

dx.doi.org/10.1021/ie501542p | Ind. Eng. Chem. Res. XXXX, XXX, XXX−XXX

Table 5. Conversion−Time Data for Various N_{AB} Samples[a]

	α				
t (s)	N_{AB} = 3	N_{AB} = 6	N_{AB} = 12	N_{AB} = 17	N_{AB} = 41
0	0	0	0	0	0
2700	0.43	0.41	0.38	0.40	0.46
	0.41			0.42	
3600	0.61	0.58	0.50	0.40	0.60
	0.62			0.39	
4500	0.69	0.66	0.59	0.60	0.65
	0.70			0.64	
6300	0.69	0.69	0.65	0.65	0.68
8100	0.79	0.80	0.77	0.73	0.79
	0.81			0.6	
9900	0.84	0.84	0.81	0.82	0.84
	0.85			0.80	

[a]For certain cases, the experiments were repeated to check the reproducibility and the duplicate results are shown.

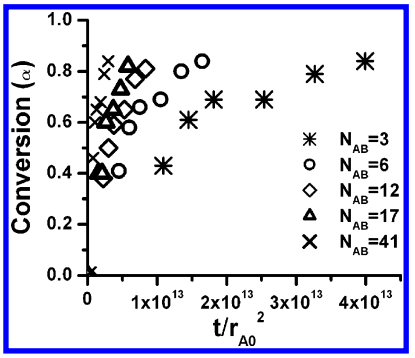

Figure 4. Plot of conversion versus t/r_{A0}^2 for different N_{AB} values showing the effect of N_{AB} on kinetics.

$$I_1(\xi) = I(\xi) - I(\xi_0) = \int_{\xi_0}^{\xi} S(\bar{\xi}) \int_{\xi_1}^{\bar{\xi}} \frac{dr}{S(r)} d\bar{\xi}$$
$$= \frac{D}{K}(t - t_0) + C \quad (14)$$

where ξ_0 is the position of the reaction front at t_0, calculated from the measured conversion at that time, and C is a constant that depends on the progress of the reaction during the nonisothermal period.

In eq 14, the inner integral can be evaluated analytically as described earlier. A trapezoidal rule was used to calculate the integral $I_1(\xi)$ for different times. For this purpose, the value of ξ was calculated for each time from the measured conversion. The relationship between α and ξ in the phase 1 is given by[4]

$$\alpha = N_{AB}\left(0.5\frac{\xi^3}{r_{A0}^3} - 0.1875\frac{\xi^4}{r_{A0}^4}\right) \quad (15)$$

Equation 15 was solved for ξ using the solver tool available in MS Excel, which uses the generalized reduced gradient (GRG2) algorithm.[22] In the calculation of $I_1(\xi)$, a value of $\xi_1 = 0.05r_{A0}$ was assumed, following Shimizu and Hao.[7] It was noted in the previous work of Dalvi and Suresh[4] and confirmed by calculations in this work that conversion−time curves calculated using the model are independent of D and ξ_1 as long as the product $D\xi_1$ is constant. In other words, if ξ_1 is regarded as a parameter, it is only the product $D\xi_1$ that can be estimated from single N_{AB} data points. The value of ξ_1 presumably depends on several factors, including the pelletization conditions (such as the particle sizes of reactants and the pressure applied for compaction) and reaction conditions.

Values of $I_1(\xi)$ thus calculated for phase 1 of the reaction are plotted as a function of $(t - t_0)/K$ for N_{AB} values of 6, 12, and 17, together with the best-fit straight line in each case, in Figure 5. Reasonable straight-line fits can be seen. The estimated value

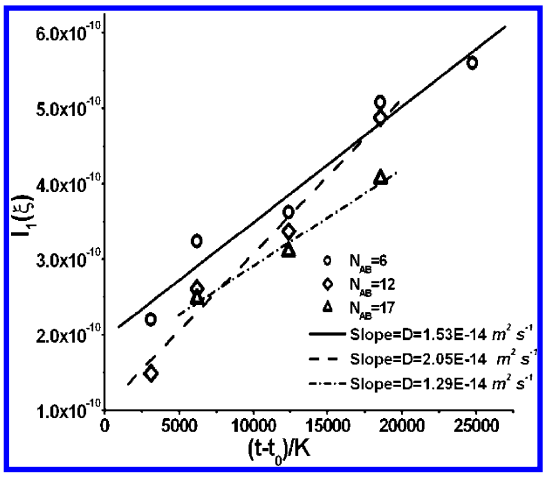

Figure 5. Linear fitting to the experimental $I_1(\xi)$ vs $(t - t_0)$ data for the estimation of D (eq 14).

of the parameter $D\xi_1$, as well as D values calculated for the assumed value of ξ_1 for comparison, are reported in Table 6. Although the values do show some scatter, no systematic dependence on N_{AB} can be seen.

In Figure 6, the data for all N_{AB} values are plotted in accordance with the Ginstling and Brownshtein (GB) model (eq 13). It can be seen that this model also fits the data reasonably well. A reference to the literature[1,2,13] shows that, for solid−solid reaction kinetics, it is not unusual to find different models fitting the data equally well. However, the calculated D values in this case (see Table 6) show a systematic dependence on N_{AB}, increasing with the value of N_{AB}. The estimated values are generally smaller than those estimated by the Dalvi−Suresh model[4] for all values of N_{AB}.

Ghoroi and Suresh[2] studied the formation of C_3A from $CaCO_3$ and $C_{12}A_7$ and estimated a value of $D = 1.05 \times 10^{-15}$ m^2 s^{-1} using the Hao−Tanaka model[5] and assuming the same value for ξ_1 as in this work. Dalvi−Suresh[4] re-estimated D for the data of Ghoroi and Suresh using their model as 3.579×10^{-16} m^2 s^{-1}. Table 7 reports these values, along with values obtained using conventional models from two studies in the literature on systems similar to ours.

Comparing these values and our estimates from the Dalvi−Suresh model in Table 6, one can see a considerable variation in the order of magnitude of the values, with the values from this study falling somewhere in the middle. As Table 7 (also see Table 2) shows, there are significant differences in powder characteristics between the previous study[2] and the present study on the same system. The reactant powders used in the experiments of Ghoroi and Suresh[2] had a wide range of sizes (and the values of N_{AB} were calculated using average values), whereas in the present study, care was taken to use narrow size fractions of the reactant powders. The application of contact-point models in situations in which particle sizes (and hence N_{AB}) are distributed requires careful consideration, and use of an average size might not be the right approach. Also, the particle sizes in Ghoroi and Suresh[15] were much smaller than those used

dx.doi.org/10.1021/ie501542p | Ind. Eng. Chem. Res. XXXX, XXX, XXX−XXX

Table 6. Comparison of D Values Estimated According to the Dalvi−Suresh[4] and Ginstling−Brounshtein[15] Models[a]

	Dalvi−Suresh model[4]			Ginstling−Brounshtein model[15]	
N_{AB}	$D\xi_1$ ($\times 10^{-20}$ m^3 s^{-1})	R^2	D ($\times 10^{-14}$ m^2 s^{-1})	D ($\times 10^{-16}$ m^2 s^{-1})	R^2
3				5.30	0.961
6	1.91	0.979	1.53	12.7	0.972
12	3.54	0.986	2.05	21.7	0.964
17	2.68	0.992	1.29	30.8	0.970
41			–	69.8	0.977
mean	2.71		1.62		–

[a]Calculation of D values by the Dalvi−Suresh model assumes $\xi_1 = 0.05 r_{A0}$.

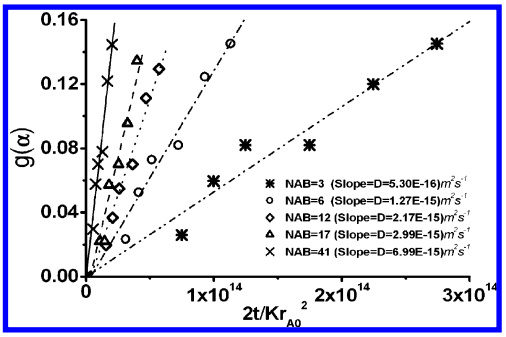

Figure 6. Linear fitting of data in accordance with the GB model (eq 13).

in this study, with the result that the ratio of surface area to volume of $C_{12}A_7$ used was 10 times larger in their study. Furthermore, the particle size of CaO reactant was unknown in their experiments as only the size of the precursor $CaCO_3$ was reported. The difference in measured D values can be attributed to these reasons. Further, it can be observed that, subject to any small uncertainty in the value of ξ_1 assumed, the estimated diffusion coefficient in this present study falls within the range of ^{45}Ca diffusion obtained in many polycrystalline oxides.[23,24]

4.1. Validation of the Model for the Cases of N_{AB} = 41 and N_{AB} = 3. The case of N_{AB} = 41 was chosen for experiments because, at such values, the particle goes through all three phases over the conversion range measured (see Tables 4 and 5), and that of N_{AB} = 3 provides an opportunity to study a very-low-N_{AB} case, covering two phases in its conversion range. With values of $D\xi_1$ determined from the phase 1 data above, we can therefore examine how the model performs in a case in which all phases are represented in the data. Use of the model for such situations is described by Dalvi and Suresh.[4] Equations 4−6 were used to obtain $i(\xi)$, and the final integration shown in eq 14 was carried out using the "Quad" function in MATLAB.[26]

Figure 7 shows a comparison between the calculated (using the mean value of $D\xi_1$ estimated above) and experimental

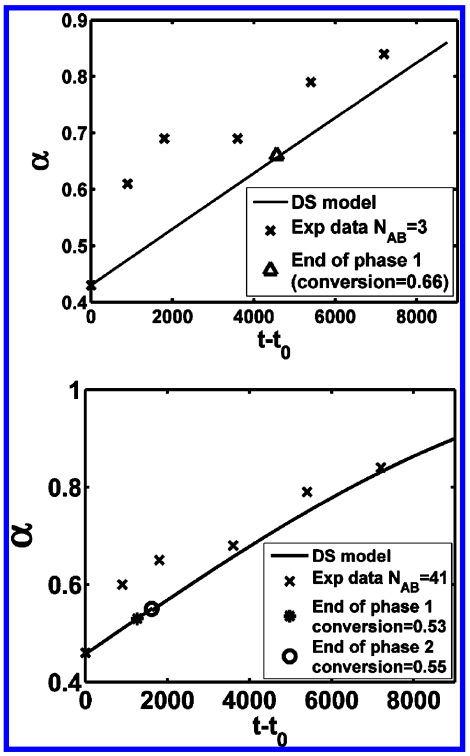

Figure 7. Comparison of experimental data for N_{AB} = 3 and N_{AB} = 41 with simulated curves, with $D\xi_1 = 2.71 \times 10^{-20}$ m^2 s^{-1}. The points marking the ends of phases I and II of the reaction are also shown.

conversions for N_{AB} = 41 and N_{AB} = 3. The fit for the former case is better than that for the latter case. It may be recalled that Dalvi and Suresh[4] derived special equations for small N_{AB}.

Table 7. Reported Values for the Diffusion Coefficient of Ca in Polycrystalline Oxides and Comparison with the Present Study

	formation of C_3A		formation of CA	
	present study data using the Dalvi−Suresh[4] model	Ghoroi and Suresh[2] by the Dalvi−Suresh[4] model	Ali et al.[25]	^{45}Ca in Al_2O_3[23,24]
particle size of CaO (μm)	31.5 (range 25−38), CaO	2.52, (range 0.5 to 12), $CaCO_3$	–	–
particle size of $C_{12}A_7$ (μm)	315 (range 25−38)	1.77, (range 0.5 to 8)	–	–
surface area/volume ratio of $C_{12}A_7$[a] (m^2/m^3)	(2.81−4.27) $\times 10^5$ (average 3.33 $\times 10^{05}$)	(1.33 $\times 10^6$)−(2.13 $\times 10^7$)	–	–
reported N_{AB}	3	2	–	–
temperature (K)	1523	1523	1523	1670
estimated D (m^2 s^{-1})	1.62 $\times 10^{-14}$	3.579 $\times 10^{-16}$	2.13 $\times 10^{-12}$	3.1 $\times 10^{-13}$

[a]Assuming spherical particles.

dx.doi.org/10.1021/ie501542p | Ind. Eng. Chem. Res. XXXX, XXX, XXX−XXX

Although the fits in both cases can be considered reasonable within the limits of experimental error, it must be said that the special models for low N_{AB} bear further comparison with experimental data. It must also be noted that the predictions from the model are dependent on the measured value of conversion at the start of the isothermal period.

A reference to Tables 4 and 5 shows that N_{AB} values 12 and 17 contain some high-conversion data that fall in phase 2 (these data were therefore omitted in the estimation of D). A prediction of the conversion using the D value estimated above gives values within 12−13% of the measured values. Taken together, the body of evidence thus seems to validate the Dalvi−Suresh model.

5. CONCLUSIONS

A new method for interpreting solid−solid reaction kinetics based on the contact-point based model of Dalvi and Suresh[4] has been proposed in this work. It was shown that the conventional models (that of Ginstling−Brounshtein being a representative case) would predict different values of diffusivity at the same temperature depending on the number of contact points N_{AB}, whereas the Dalvi−Suresh model estimates consistent values. Although it is true that a value of ξ_1 needs to be assumed to derive a value of D, $D\xi_1$ itself can be regarded as a parameter, and as long as the pellet preparation and reaction conditions do not change, it can be estimated from laboratory experiments and used in design. It might also be possible to estimate ξ_1 separately, and strategies to do this are under investigation. Assuming a value of $\xi_1 = 0.05r_{A0}$ as suggested in the literature, we estimate the diffusivity D to be on the order of $\sim 10^{-14}$ m^2 s^{-1} at 1250 °C, which is similar to the diffusivity values expected for Ca in polycrystalline solids.

Thus, it appears that the model proposed by Dalvi and Suresh[4] is more suitable than the continuum models traditionally employed to describe solid−solid reactions. Further validation of the Dalvi−Suresh model has been provided by testing the prediction of the model for low (3) and high (41) values of N_{AB}.

AUTHOR INFORMATION

Corresponding Author

*E-mail: aksuresh@iitb.ac.in.

Present Address

†PDA College of Engineering, Gulbarga, Karnataka, India.

Notes

The authors declare no competing financial interest.

ACKNOWLEDGMENTS

The authors thank the Department of Metallurgy and Materials Science, IIT Bombay, for permission to use their XRD facility.

NOTATION

A = nondiffusing reactant in a binary mixture ($C_{12}A_7$)
a = number of moles of reactant A
B = diffusing reactant in a binary mixture (CaO)
b = number of moles of reactant B
$C_{12}A_7 = Ca_{12}Al_{14}O_{33}$
$C_3A = Ca_3Al_2O_4$
D = effective diffusivity of reactant B in reactant A, m^2 s^{-1}
$K = b\rho_A/a\rho_B$
R^2 = correlation coefficient
r_{A0} = radius of reactant A, m
r_{B0} = radius of reactant B, m
R_m = molar ratio = m_B/m_A
R_r = initial radius ratio = r_{B0}/r_{A0}
R_ρ = ratio of molar densities of reactants = ρ_B/ρ_A
t = time, s

Greek Symbols

α = conversion
ε = volume fraction of porosity
ε_a = surface fraction of porosity, $1 - (2/13)(7 - 8\varepsilon)$
ξ = reaction front radius, m
$\xi_1 = 0.05r_{A0}$
ρ_A = molar density of reactant A
ρ_B = molar density of reactant B

REFERENCES

(1) Ghoroi, C.; Suresh, A. K. Solid−Solid Reaction Kinetics: Formation of Tricalcium Aluminate. *AIChE J.* **2007**, *53*, 502−513.
(2) Ghoroi, C.; Suresh, A. K. Intermediate Conversion Kinetics in Ticalcium Aluminate Formation. *AIChE J.* **2007**, *53*, 2399−2410.
(3) Suresh, A. K.; Ghoroi, C. Solid−Solid Reactions in Series: A Modeling and Experimental Study. *AIChE J.* **2009**, *55*, 2399−2413.
(4) Dalvi, V. V.; Suresh, A. K. A Contact-Point Based Approach for the Analysis of Reactions among Solid Particles. *AIChE J.* **2011**, *57*, 1329−1338.
(5) Hao, Y. J.; Tanaka, T. Role of the Contact Points between Particles on the Reactivity of Solids. *Can. J. Chem. Eng.* **1988**, *66*, 761−766.
(6) Ouchiyama, N.; Tanaka, T. Estimation of the Average Number of Contacts between Randomly Mixed Solid Particles. *Ind. Eng. Chem. Fundam.* **1980**, *16*, 338−340.
(7) Shimizu, A.; Hao, Y. Influence of Particle Contact on the Estimation of Powder Reaction Kinetics of Binary Mixtures. *J. Am. Ceram. Soc.* **1997**, *80*, 557−568.
(8) Shimizu, A. Suitability of the Kinetic Model for Estimation of Powder Reaction Rate. *Powder Technol.* **1998**, *100*, 24−31.
(9) Lutterotti, L. Total Pattern Fitting for the Combined Size−Strain−Stress−Texture Determination in Thin Film Diffraction. *Nucl. Instrum. Methods Phys. Res. B: Beam Interact. Mater. Atoms* **2010**, *268*, 334−340.
(10) Rietveld, H. M. Line Profiles of Neutron Powder-Diffraction Peaks for Structure Refinement. *Acta Crystallogr.* **1967**, *22*, 151−152.
(11) Rietveld, H. M. A Profile Refinement Method for Nuclear and Magnetic Structures. *J. Appl. Crystallogr.* **1969**, *2*, 65−71.
(12) Mohamed, B. M.; Sharp, J. H. Kinetics and Mechanism of Formation of Monocalcium Aluminate, $CaAl_2O_4$. *J. Mater. Chem.* **1997**, *7*, 1595−1599.
(13) Mohamed, B. M.; Sharp, J. H. Kinetics and Mechanism of Formation of Tricalcium Aluminate, $Ca_3Al_2O_6$. *Thermochim. Acta* **2002**, *388*, 105−114.
(14) Iftekhar, S.; Grins, J.; Svensson, G.; Loof, J.; Jarmar, T.; Gianluigi, A.; Carmen, M.; Engqvist, H. Phase Formation of $CaAl_2O_4$ from $CaCO_3$−Al_2O_3 Powder Mixtures. *J. Eur. Ceram. Soc.* **2008**, *28*, 747−756.
(15) Ginstling, A. M.; Brounshtein, B. L. Concerning the Diffusion Kinetics of Reactions in Spherical Particles. *Appl. Chem. USSR* **1950**, *23*, 1327−1338.
(16) Chincho, S. Quantitative Rietveld Analysis of Aluminous Cement Clinker Phases. *Cem. Concr. Res.* **2000**, *30*, 1023−1029.
(17) Hillier, S. Accurate Quantitative Analysis of Clay and Other Minerals in Sandstones by XRD: Comparison of a Rietveld and a Reference Intensity Ratio (RIR) Method and the Importance of Sample Preparation. *Clay Miner.* **2000**, *35*, 291−291.
(18) Lapovok, R.; Tomus, D.; Skripnyuk, V. M.; Barnett, M.; Gibson, M. A. The Effect of Hydrogenation on the ECAP Compaction of Ti-6Al-4V Powder and the Mechanical Properties of Compacts. *Mater. Sci. Eng., A* **2009**, *513*−*514*, 97−108.

(19) Guirado, F.; Galí, S. Quantitative Rietveld Analysis of CAC Clinker Phases Using Synchrotron Radiation. *Cem. Concr. Res.* **2006**, *36*, 2021−2032.
(20) Balonis, M.; Glasser, F. P. The Density of Cement Phases. *Cem. Concr. Res.* **2009**, *39*, 733−739.
(21) Tas, A. C. Chemical Preparation of the Binary Compounds in the Calcia−Alumina System by Self-Propagating Combustion Synthesis. *J. Am. Ceram. Soc.* **1998**, *81*, 2853−2863.
(22) Daniel, F.; Lasdon, L.; Watson, J.; Warren, A. Design and Use of the Microsoft Excel Solver. *Interfaces* **1998**, *28*, 29−55.
(23) Freer, R. Bibliography. Self-Diffusion and Impurity Diffusion in Oxides. *J. Mater. Sci.* **1980**, *15*, 803−824.
(24) Harrop, P. J. Self-Diffusion in Simple Oxides (A Bibliography). *J. Mater. Sci.* **1968**, *3*, 206−222.
(25) Ali, M. M.; Agarwal, S. K.; Handoo, S. K. Difffusion Studies in Formation and Sintering of $CaAl_2O_4$ and $BaAl_2O_4$: A Comparative Evaluation. *Cem. Concr. Res.* **1997**, *27*, 979−982.
(26) Gander, W.; Gautschi, W. Adaptive Quadrature—Revisited. *BIT Numer. Math.* **2000**, *40*, 84−101.